ADVANCED HEALTHCARE MATERIALS
www.advhealthmat.de

Self-Adjuvanted Molecular Activator (SeaMac) Nanovaccines Promote Cancer Immunotherapy

Zichao Luo, Tao He, Peng Liu, Zhigao Yi, Shunyao Zhu, Xiuqi Liang, Entang Kang, Changyang Gong, and Xiaogang Liu**

Neoantigen-based immunotherapy is a promising treatment option for many types of cancer. However, its efficacy and abscopal effect are limited by impotent neoantigens, high treatment costs, and complications due to action of adjuvants. Here, the design and synthesis of nanovaccines are reported, based on self-adjuvanted, polymer nanoparticles with in vivo neoantigen-harvesting and molecular activating capabilities. These nanovaccines inhibit tumor growth significantly and prolong the survival of tumor-bearing mice in both colon carcinoma 26 (CT26) and B16-F10 tumor models. Mechanistic studies suggest that as-synthesized nanovaccines can promote dendritic cell maturation and accumulation expeditiously in lymph nodes, leading to the expansion of cytotoxic $CD8^+$ T cells. Moreover, these nanovaccines elicit abscopal effects in CT26 and B16-F10 tumors without the need for adjuvants or immune checkpoint inhibitors. Combined with an anti-PD-L1 antibody, nanovaccines can evoke robust, long-term memory immune response, as evidenced by tumor growth inhibition and high survival rates (~ 67%) over 90 days. These results highlight the potential of using self-adjuvanted nanovaccines as a simple, safe, and affordable strategy to boost neoantigen-based cancer immunotherapy.

1. Introduction

Immunotherapy is considered the fourth pillar of cancer treatments, along with surgery, chemotherapy, and radiotherapy.[1] Cancer immunotherapies, including cancer vaccines, immune checkpoint inhibitors (anti-CTLA-4, anti-PD-1, and anti-PD-L1 antibodies), and chimeric antigen receptor T cell therapies, can extend survival in patients with advanced disease.[2] In particular, cancer vaccines comprising tumor-associated antigens (TAAs) and adjuvants have proven effective in inducing TAA-specific T cells and antibodies in preclinical and clinical trials.[3] However, TAA-based cancer vaccines face two notable challenges: a slow immune response rate due to low-affinity interactions with T cells and non-discriminative overexpression in tumor and healthy tissues.[4] To tackle these challenges, tumor neoantigens, arising from non-synonymous mutations and genetic alterations without expression in healthy tissues, have been widely used in neoantigen-based vaccine development.[4]

Tumor neoantigen-specific $CD4^+$ T and $CD8^+$ T cells, reactive to respective neoantigen MHC-II and MHC-I epitopes, are essential to inhibit tumor growth in various murine tumor models, including colon carcinoma 26 (CT26), 4T1 mammary carcinoma, B16-F10 melanoma, d42m1-T3, and F244 sarcoma tumors.[5] Importantly, personalized cancer vaccines, based on combinations of adjuvants and predicted HLA class-II or class-I neoantigens, elicit substantial neoantigen-specific $CD4^+$ and $CD8^+$ cytolytic T cell responses, resulting in complete or partial tumor regression in a variety of malignant diseases.[6] Compared with TAAs, neoantigen-based cancer vaccines offer more specific immunogenicity in both preclinical studies and clinical trials. Neoantigen-based vaccines also provide excellent safety profiles but require time-consuming identification of immunogenic neoantigens, which remains a challenging task. Another constraint associated with neoantigen-based therapies is the need for adjuvant mixing (e.g., polyinosinic–polycytidylic acid (PIC), CpG oligodeoxynucleotide (CpG), Monophosphoryl Lipid A (MPLA)) to boost immune responses, thus adding complexity and cost to cancer treatment.

Here, we report the design of self-adjuvanted molecular activator (SeaMac) nanovaccines for enhanced cancer immunotherapy.

Z. Luo, Dr. Z. Yi, Dr. X. Liu
Department of Chemistry and The N.1 Institute for Health
National University of Singapore
Singapore 117543, Singapore
E-mail: chmlx@nus.edu.sg
Dr. T. He, S. Zhu, X. Liang, Prof. C. Gong
State Key Laboratory of Biotherapy and Cancer Center
West China Hospital
Sichuan University
Chengdu 610041, P. R. China
E-mail: chygong14@163.com
Dr. P. Liu, Prof. E. Kang
Department of Chemical and Biomolecular Engineering
National University of Singapore
Singapore 117585, Singapore
Dr. X. Liu
Joint School of National University of Singapore and Tianjin
University International Campus of Tianjin University
Fuzhou 350207, P. R. China

The ORCID identification number(s) for the author(s) of this article can be found under https://doi.org/10.1002/adhm.202002080

DOI: 10.1002/adhm.202002080

SeaMac nanovaccines have two essential characteristics: one is the ability to harvest neoantigens at nanoparticle surfaces from perished tumor cells, and the other is to induce dendritic cell (DC) maturation through stimulator of interferon genes (STING) (Figure S1, Supporting Information). SeaMac nanovaccines have a maleimide moiety capable of harvesting neoantigens through the Michael reaction between thiol and maleimide groups. Meanwhile, C7A monomers, designed to constitute the inner core of SeaMac nanovaccines, can promote DC maturation and improve downstream antigen presentation and T cell activation.[7] Unlike conventional neoantigen-based cancer vaccines, SeaMac nanovaccines enable high-efficiency personalized therapy, because they can harvest neoantigens from perished tumor cells and present neoantigens to $CD8^+$ T cells while inducing DC maturation. These activated $CD8^+$ T cells could participate in inhibiting primary and distant tumors. For this reason, we reasoned that SeaMac nanovaccines might provide a powerful strategy for cancer treatment without constraints associated with conventional methods.

2. Results and Discussion

As proof of concept, we designed and synthesized self-adjuvanted and neoantigen-harvesting Mal-PEG_{5000}-*b*-$PC7A_{45}$ nanoparticles (described as Mal-NPs), while NH_2-PEG_{5000}-*b*-$PC7A_{45}$ nanoparticles (defined as NH_2-NPs) were prepared as a control. For Mal-NPs synthesis, an amphiphilic block polymer (Boc-PEG_{5000}-*b*-$PC7A_{45}$) was firstly synthesized by reversible addition–fragmentation chain transfer polymerization of C7A through the use of Boc-PEG_{5000}-CDTPA as the macro chain transfer agent. Subsequently, NH_2-PEG_{5000}-*b*-$PC7A_{45}$ polymer was obtained by removing the Boc group of Boc-PEG_{5000}-*b*-$PC7A_{45}$ polymer using trifluoroacetic acid. Finally, 6-maleimidohexanoic acid was conjugated to NH_2-PEG_{5000}-*b*-$PC7A_{45}$ using 1-Ethyl-3-[3-dimethylaminopropyl]cabodiimide and *N*-hydroxysuccinimide as coupling agents to obtain Mal-PEG_{5000}-*b*-$PC7A_{45}$ polymer (Figure S2, Supporting Information). Chemical structures of all three polymers were characterized by ^1H NMR, gel permeation chromatography, fluorescence spectroscopy, and Fourier-transform infrared spectroscopy (Figure S3 and Table S1, Supporting Information). NH_2-NPs and Mal-NPs were prepared by self-assembly of amphiphilic NH_2-PEG_{5000}-*b*-$PC7A_{45}$ and Mal-PEG_{5000}-*b*-$PC7A_{45}$, respectively, in PBS (pH 7.6) (**Figure 1**a,b). The spherical morphology and particle size (~ 60 nm) of NH_2-NPs and Mal-NPs were confirmed by transmission electron microscopy (Figure 1c). They both have a hydrodynamic size of ~ 100 nm in phosphate-buffered saline (PBS) solution, as determined by dynamic light scattering (Figure 1d). Moreover, NH_2-NPs are more positively charged than Mal-NPs (Figure 1e).

DCs, the most potent professional antigen present cells (APCs), play a critical role in mediating innate response and inducing adaptive immune response.[8] Previous studies indicate that C7A monomer-containing nanoparticles can deliver proteins or mRNA vaccines to elicit potent immune responses against cancer.[7,9] To examine the feasibility of NH_2-NPs- and Mal-NPs-induced DC maturation *in vitro*, we evaluated cytotoxic effects of NH_2-NPs and Mal-NPs against 3T3 and Raw 264.7 cells using the standard MTT assay. Cell viabilities were over 90% in both cell lines, even at a particle concentration of 400 μg mL^{-1}, indicating excellent biocompatibility (Figure S4, Supporting Information). Bone marrow DCs (BMDCs) were then treated with blank NH_2-NPs and Mal-NPs at 50 μg mL^{-1} for 24 h, and expressions of co-stimulatory molecules were determined using flow cytometry. Both NH_2-NPs and Mal-NPs promoted BMDC maturation, as evidenced by approximately two- fold enhanced expressions of CD80, CD83, and CD86 compared with the medium (Figure 1f–h, and Figure S4, Supporting Information). Notably, both NH_2-NPs and Mal-NPs enhanced TNF-a markedly, but with a slight improvement in IL-1β production (Figure 1i,j). The mechanism of this effect can be ascribed to the activation of STING by C7A monomers, as demonstrated in STING knockout mice.[7] Taken together, these results suggest the suitability of both NH_2-NPs and Mal-NPs as adjuvants in tumor immunotherapy.

Next, we evaluated the ability of Mal-NPs to capture released neoantigens from perished tumor cells *in vitro*. First, a standard photodynamic therapy (PDT) protocol based on chlorin e6 (Ce6)-conjugated upconversion nanoparticles (UCNPs) was adopted to generate perished tumor cells (**Figure 2**a and Figure S5, Supporting Information). For PDT, UCNP-SiO_2-Ce6 (denoted as UCNP-Ce6) was synthesized and characterized by TEM, UV–Vis spectroscopy, and fluorescence spectroscopy (Figure S5, Supporting Information). Under 980-nm irradiation, UCNP-Ce6 produced reactive oxygen species *in vitro*, inducing around 30% apoptosis in both B16-F10 and CT26 tumor cells (Figure S5, Supporting Information). Then, NH_2-NPs and Mal-NPs were treated with B16-F10 melanoma cell lysates induced by PDT *in vitro*. Total tumor-derived protein antigens were quantified by measuring the amount of proteins bound to each NP. Mal-NPs harvested more proteins than NH_2-NPs, consistent with a previous study (Figure 2b).[10] NH_2-NPs and Mal-NPs formulations showed a similar ability to capture a comprehensive set of proteins (Figure 2c). Notably, among approximately 730 sets of proteins captured, NH_2-NPs showed 91 unique sets, while Mal-NPs displayed 108 unique sets (Figure 2d). Subsequently, an in silico analysis was performed to confirm the existence of neoantigens in captured proteins, as expressed by B16-F10 cells.[5a,11] Although NH_2-NPs and Mal-NPs both captured eight sets of neoantigens, Mal-NPs harvested several sets of neoantigens (e.g., Ppp1r7, Dag1and Actn4) with a much higher density (Figure 2e, Figure S6 and Table S2, Supporting Information). The captured neoantigens, such as Actn4, Eef2, and Dag1, enhanced tumor immunotherapy in an antigen-specific manner, as demonstrated by a potent IFN-γ production *ex vivo* after neoantigen stimulation.[10] Moreover, this improvement may be also associated with an abundance of the captured neoantigens.[10] Notably, both types of nanoparticles can capture damage-associated molecular pattern proteins (DAMPs), which are pro-inflammatory biomolecules known to improve immune responses.[12] Notably, Mal-NPs captured a significantly higher density of DAMPs than NH_2-NPs, such as the heat shock protein (Hsp) family (Hsp90ab1, Hspa11, Hspa5, Hsp8, and Hspd1), the histone protein family (Hist1h2ap and Hist2h2bb), and alarmins (Hmgb1), all of which have shown enhanced immune responses against tumor[12] (Figure 2e, Figure S6 and Table S2, Supporting Information). Overall, our data suggest that Mal-NPs show a stronger capacity for neoantigens and DAMPs released from irradiated B16-F10 cells.

The antigen uptake and presentation by APCs, such as DCs, macrophages, and B cells, is the initial step of vaccine-induced

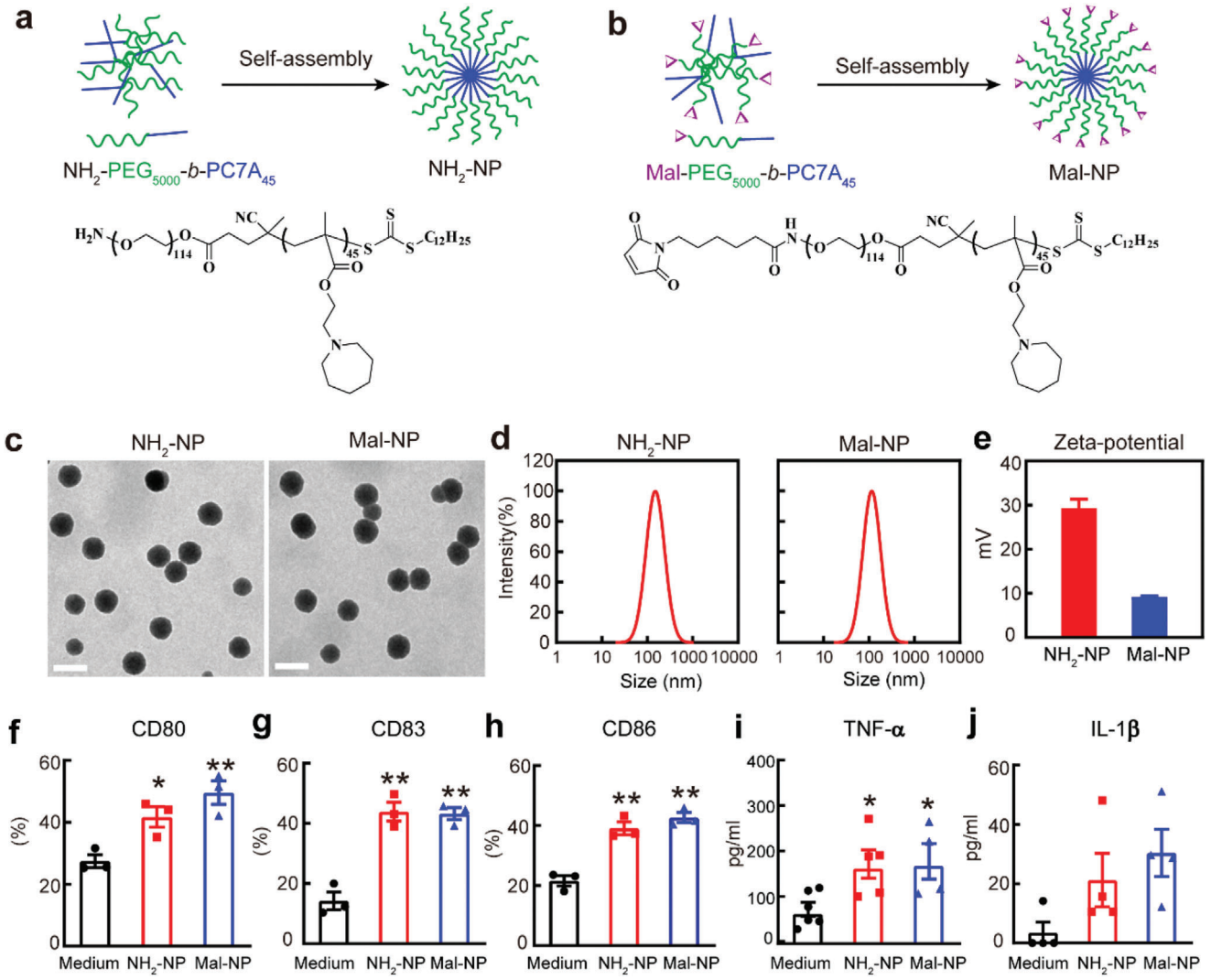

Figure 1. Mal-NPs promote maturation of mouse bone marrow BMDCs through the STING signal pathway. a,b) Schematic self-assembly of NH_2-PEG_{5000}-*b*-$PC7A_{45}$ and Mal-PEG_{5000}-*b*-$PC7A_{45}$ polymers into nanoparticles. c) TEM images of NH_2-NPs and Mal-NPs. Scale bar, 100 nm. d,e) Size and zeta-potential of NH_2-NPs and Mal-NPs in PBS buffer (pH at 7.6). f–h) Impact levels of NH_2-NPs and Mal-NPs on CD80, CD83, and CD86 expression using bone marrow BMDCs. i,j) Impact levels of NH_2-NPs and Mal-NPs on TNF-a and IL-1β production using BMDCs. Values are means ± s.e.m. (n = 3–4 biologically independent samples; asterisk: medium versus other treatments, *$p < 0.05$; **$p < 0.01$; one-way ANOVA analysis with Tukey test).

adaptive immunity in lymph nodes.[13] To study whether NH_2-NPs or Mal-NPs can deliver neoantigens and DMAPs to APCs, we injected 1,1′-dioctadecyl-3,3,3′,3′-tetramethylindodicarbocyanine (DiD)-labeled NH_2-NPs or DiD-labeled Mal-NPs intratumorally two days after PDT. We studied particle lymphatic drainage and distribution in B cells, macrophages, and DCs residing in tumor-draining lymph nodes (TDLNs) 16 h after post-injection (Figure 2f). Mal-NPs were accumulated in DCs ($CD11c^+$) and B cells ($B220^+$) at higher rates than NH_2-NPs, whereas the accumulation rates of the two nanoparticles in macrophages were similar (Figure 2f and Figure S7, Supporting Information). Furthermore, PDT markedly enhanced Mal-NPs uptake by both DCs and B cells in TDLNs (Figure S7, Supporting Information), similar to a previous study.[10]

Considering that Mal-NPs capture neoantigens, accumulate in lymph nodes, and promote DC maturation, we next investigated the effect of Mal-NPs on tumor immunotherapy in B16-F10 and CT26 tumor models. Mice bearing CT26 or B16-F10 tumors in the right flank underwent PDT on day 7 (**Figure 3**a). Two days later, mice were intratumorally immunized with NH_2-NPs or Mal-NPs three times at a 2-day interval. The treatment efficacy was evaluated by monitoring tumor volume and survival time. In the CT26 tumor model, PDT alone only slightly inhibited tumor growth, while NH_2-NPs-based PDT showed moderate antitumor activity. In contrast, Mal-NPs-based PDT led to more pronounced inhibition of tumor growth, as assessed by measuring the tumor volume across all groups over 24 days (Figure 3b). The survival rate of mice in the PDT/Mal-NPs group reached 30% on day 37, while all mice from other groups died within 35 days (Figure 3c). Mice were euthanized on day 24, and tumors were harvested and weighed. Tumors taken from PDT/NH_2-NPs and PDT/Mal-NPs groups showed 63.9% and 82.3% reduction in weight,

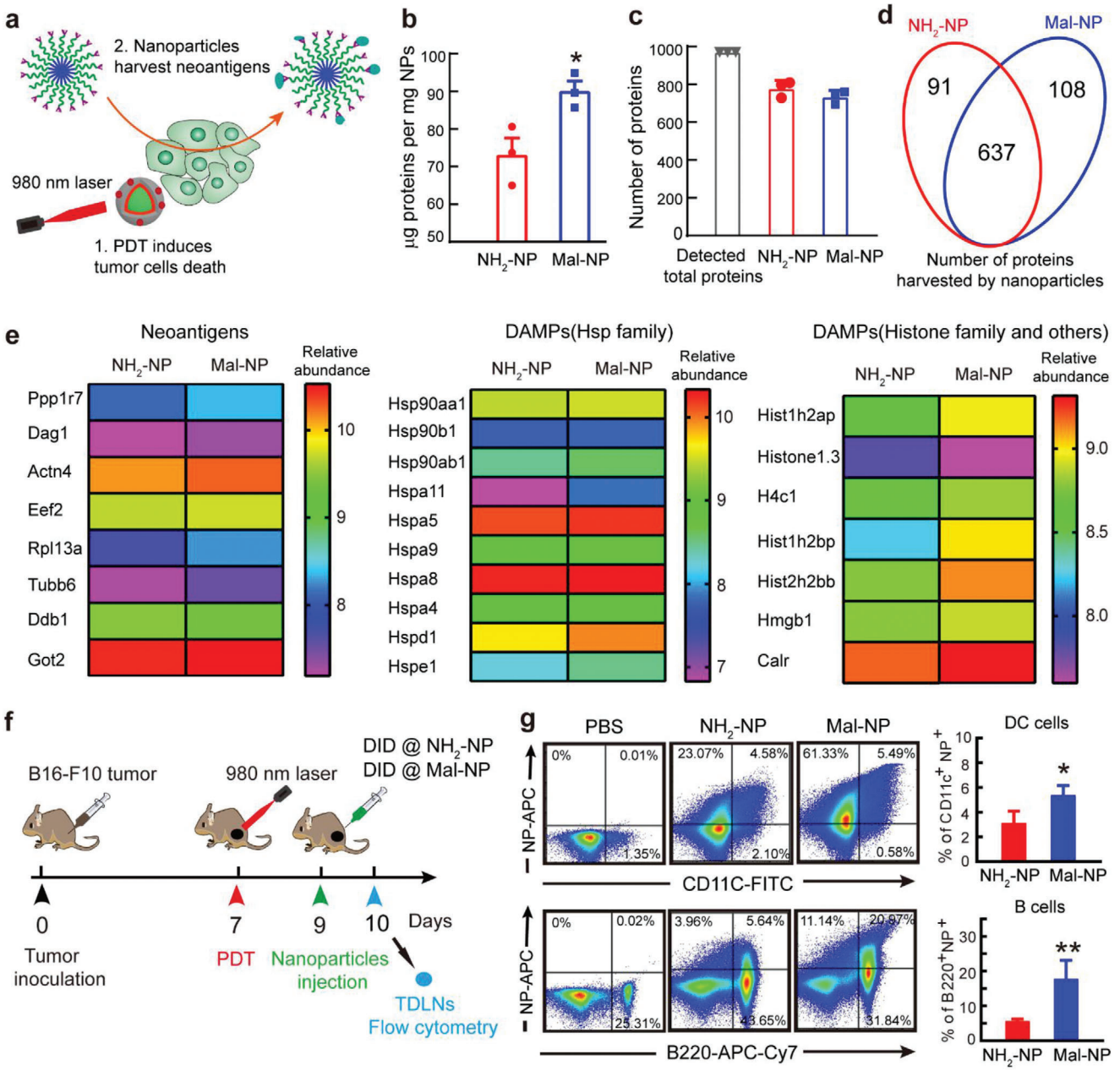

Figure 2. Mal-NPs harvest neoantigens and promote cellular uptake in lymph node-resident immune cells. a) Schematic illustration of neoantigen harvesting using NH_2-NPs and Mal-NPs. b) Quantification of proteins harvested by NH_2-NPs and Mal-NPs using the Bicinchoninic Acid Protein Assay kit. c) The total number of proteins harvested by NH_2-NPs and Mal-NPs. d) Comparison of the number of proteins harvested by NH_2-NPs and Mal-NPs. e) The heatmap of the relative abundance of neoantigens and DMAPs harvested by NH_2-NP and Mal-NP. The relative abundance represents the average value of three runs. f) Schematic timeline of DID@NH_2-NP and DID@Mal-NP *in vivo* cellular uptake. g) Flow cytometric analysis of cellular uptake of DID@NPs by DCs ($CD11c^+$) and B cells ($B220^+$) in tumor-draining lymph nodes (TDLNs). Values are means ± s.e.m. ($n = 3$ biologically independent samples; $^*p < 0.05$; $^{**}p < 0.01$; Student's *t*-test).

respectively, compared to those from the PDT group (Figure S8, Supporting Information). In the B16-F10 melanoma model, compared to PDT alone, Mal-NP-based PDT showed an improved survival rate, and tumor weight reduced 73.8% (Figure 3d,e and Figure S8, Supporting Information).

We further investigated the mechanism by which Mal-NPs improves the efficacy of tumor immunotherapy. The experimental design is the same as that for the B16-F10 melanoma inhibition study (Figure 3a). Two days after immunotherapy (on day 15), all mice were euthanized, and spleens, lymph nodes, and tumor tissues were harvested for analysis of immune cell markers or cytokines. Lymph nodes are those organs where antigen-specific immune responses occur through DC interaction with T cells.[14] DC activation, characterized by high pro-inflammatory cytokines

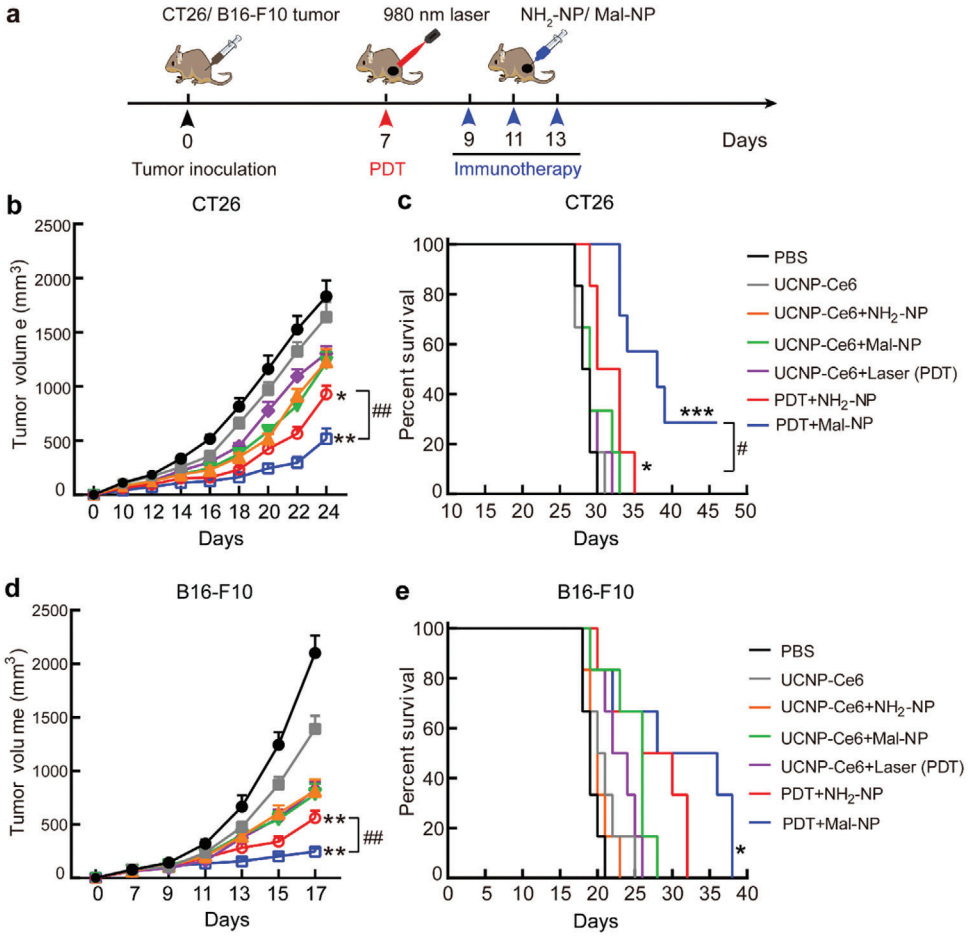

Figure 3. Mal-NPs potently inhibit both CT26 and B16-F10 tumor growth *in vivo*. a) Schematic timeline of *in vivo* tumor immunotherapy experiments. b) Average tumor growth curves of mice treated with PDT and immunotherapy in the CT26 model. c) Survival curves of mice in the CT26 tumor model (n = 6 mice per group). d) Average tumor growth curves of mice treated with PDT and immunotherapy in a B16-F10 tumor model. e) Survival curves of mice in a B16-F10 tumor model (n = 10–11 mice per group). Data represent means ± s.e.m. (asterisk: PDT versus other treatments, $^{*}p < 0.05$; $^{**}p < 0.01$; $^{***}p < 0.001$; hash: two different groups, $^{\#}p < 0.05$; $^{\#\#}p < 0.01$; tumor volume: one-way ANOVA analysis with Tukey test; survival rate: long-rank test).

and co-stimulatory expressing molecules (e.g., CD80, CD83, and CD86), is generally associated with potent and sustained activation of antigen-specific T cells.[15] Therefore, we evaluated the surface expression of CD86 and CD80 on DCs ($CD11c^+$) in TDLNs using flow cytometry. As illustrated in **Figure 4**a–c, there is an elevated cell expression (1.5–2 fold) of CD86, CD80, or double markers in TDLNs from mice treated with NH_2-NPs or Mal-NPs, compared with PBS or PDT alone. Notably, treatment of mice with Mal-NPs-based PDT results in a two-fold increase in infiltrating $CD8a^+$ DCs compared to PBS treatment, preferentially evoking a Th1 type response[16] (Figure 4d).

To confirm whether Mal-NPs-induced DC maturation in TDLNs leads to T cell activation and expansion, we analyzed the relative abundance of tumor-infiltrating help T cells ($CD3^+CD4^+CD8^-$), cytotoxic T lymphocytes (CTL, $CD3^+CD8^+CD4^-$), regulatory T cells (Treg, $CD4^+CD25^+Foxp^{3+}$), myeloid-derived suppressor cells (MDSC, $CD11b^+Ly6c^+Ly6g^+SSC^{hi}$, and $CD11b^+Ly6c^+Ly6g^-$), and activated neutrophils ($CD11b^+Ly6c^+Ly6g^+$) in B16-F10 tumors. For B16-F10 tumors treated with PDT, both NH_2-NPs and Mal-NPs injection promoted help T cell ($CD4^+$) and $CD8^+$ cytotoxic T cell (CTL) infiltration, compared with mice PBS-treated tumors (Figure 4e–g). Importantly, the percentage of $CD8^+$ CTLs in tumors after PDT/Mal-NPs treatment increased to ~ 30%, which was higher than PDT/NH_2-NP-treated groups (~12%) (Figure 4g and Figure S9, Supporting Information). Both PDT/NH_2-NPs and PDT/Mal-NPs increased the level of tumor-infiltrating Treg cells (Figure S10, Supporting Information), which is similar to a previous study.[17] One probable explanation is that the increase of Tregs is used to control inflammatory immune response induced by apoptotic cells from PDT. Notably, the PDT/Mal-NPs group induced the highest $CD8^+$ CTL/Treg ratio in tumors (Figure 4h), primarily responsible for cellular immunity due to increased antigen-specific $CD8^+$ T cells. Moreover, there were no apparent changes in levels of tumor-infiltrating-activated neutrophils ($CD11b^+Ly6c^+Ly6g^+$) (Figure 4i) and g-MDSCs ($CD11b^+Ly6c^+Ly6g^+SSC^{hi}$) in tumors across all groups (Figure S10, Supporting Information). Intratumoral treatment with PDT in combination with NH_2-NPs or Mal-NPs slightly increased the percentage of tumor-infiltrating monocytic MDSCs ($CD11b^+Ly6c^+Ly6g^-$)

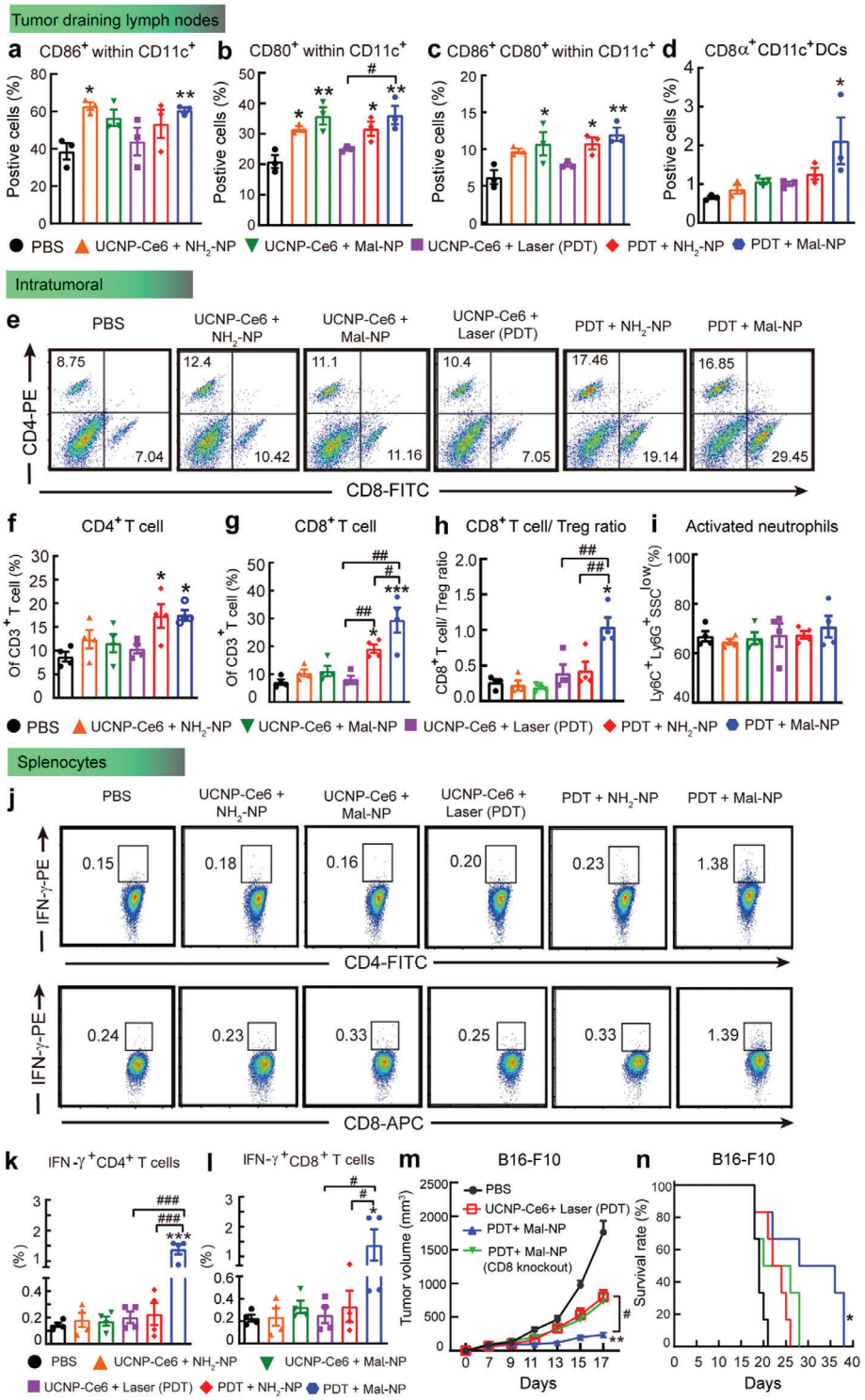

Figure 4. The immune activation mechanism of Mal-NPs on inhibition of B16-F10 tumor growth. a–c) Expression of co-stimulatory CD80 or CD86, as well as both CD80 and CD86 on DC cells ($CD11c^+$) in TDLNs of mice in a B16-F10 tumor model. d) Percent of $CD8a^+$ DC cells in TDLNs of mice in Figure 3d. e–i) The relative abundance of $CD4^+$ T cell (e,f) and $CD8^+$ T cell (e,g) subpopulations in tumors, the ratio of $CD8^+$ T cells to Treg cells (h), and the frequency of activated neutrophils (i) in tumors of mice in Figure 3d. j–l) Flow cytometric analysis assessed IFN-secreting $CD4^+$ T cells (j,k) and $CD8^+$ T cells (j,l) in the spleens of mice in B16-F10 tumor model. T cells in this assay are defined as $CD3^+$. m,n) B16-F10 tumor growth curves (m) and survival rate (n) of normal mice and CD8 T cell knockout mice treated with PDT combination with immunotherapy. All statistical data are shown as means ± s.e.m. ($n = 3$–4 biologically independent samples in a-l; $n = 6$ mice per group in (m) and (n); asterisk: PBS versus other treatments, $^*p < 0.05$; $^{**}p < 0.01$; $^{***}p < 0.001$; hash: two different groups, $^{\#}p < 0.05$; $^{\#\#}p < 0.01$; $^{\#\#\#}p < 0.001$; one-way ANOVA analysis Tukey test; survival rate: long-rank test).

relative to treatment with PBS alone.[18] The improvement in m-MDSCs may be indicative of a regulatory response to restrict STING-mediated inflammation.[19]

We next evaluated the effect of PDT/Mal-NPs on systemic T cell activation by assessing tumor-specific interferon-γ (IFN-γ) secreting splenocytes, which were stimulated with tumor lysates *ex vivo*. The highest levels of IFN-γ-secreting $CD4^+$ T and $CD8^+$ T cells were induced by combining PDT and Mal-NPs to augment tumor-specific immune responses (Figure 4j–l). Considering that PDT/Mal-NPs improved $CD8^+$ CTL accumulation in tumors (Figure 4h), we assumed that $CD8^+$ T cells participate in antitumor growth. To validate this hypothesis, we examined the antitumor effect of PDT/Mal-NPs in CD8 knockout mice. Effects of inhibitive tumor growth and prolonged survival were abolished in CD8 knockout mice compared to a wild-type control (**Figure** 4m,n). Imaging of H&E-stained tissue sections of major organs harvested from mice with different treatments confirmed the biocompatibility of the Mal-NPs (Figure S11, Supporting Information). Moreover, at 12, 24, and 48 h following immunotherapy, cytokine and chemokine concentrations were measured in the systemic circulation (Figure S12, Supporting Information). The results showed that Mal-NPs maintained normal cytokine and chemokine levels, confirming their utility for safe and efficacious antitumor immunity.

To evaluate whether SeaMac nanovaccines suppress distal tumor growth, two subcutaneous B16-F10 (or CT26 tumors) were subsequently established in the contralateral flank of C57 BL/6J mice (or Balb/c mice). The primary tumors were subject to different treatments (**Figure 5**a), whereas distant tumors were untreated. Combination of PDT with Mal-NPs inhibited primary tumor progression markedly in both B16-F10 and CT26 tumors compared with PDT alone or PDT/NH_2-NPs treatment (Figure 5b,d), consistent with single side tumor model shown in Figure 3b–d. For distant tumors, both PDT/NH_2-NPs and PDT/Mal-NPs combinations delayed B16-F10 and CT26 tumor growth (Figure 5c,e–g). The PDT/Mal-NPs combination appreciably prolonged survival in both B16-F10 and CT26 tumor models (Figure 5h–i), which could be attributed to treatment-induced systemic immune responses.

Immunological memory is a cardinal feature of adaptive immunity, and it relates to its ability to remember antigens from pathogens and protect against reinfection upon reencounter of the same pathogens, including tumor cells.[20] In addition, the blockade of programmed death receptor-1(PD-1) or PD-L1 can activate $CD8^+$ T cell proliferation and suppress Treg cell differentiation in clinic situations.[21] In principle, memory $CD8^+$ T cells can be divided into two subsets, central memory T cells (T_{CM}, $CD8^+CD62L^+CD44^+$) and effector memory T cells (T_{EM}, $CD8^+CD62L^-CD44^+$). T_{CM} cells locating in secondary lymphoid organs have little or no effector function but readily expand and differentiate to effector cells in response to antigenic stimulation. Different from T_{CM} cells, T_{EM} cells residing in both lymphoid and non-lymphoid tissues display immediate effector function by producing multiple cytokines, such as TNF-a and IFN-γ.[22] Considering that combination of PDT and Mal-NPs slightly enhanced the frequency of Tregs in tumors, we argued that introducing of anti-PD-L1 antibody into this treatment may boost a more potent and durable antitumor immune response. In this regard, mice cured of CT26 tumors were rechallenged on day 20 with the same CT26 tumors (Figure S13, Supporting Information). Effector memory $CD8^+$ T cells (T_{EM}) and central memory T cells (T_{CM}) in spleens were analyzed on day 20 in different groups of mice. The percentage of T_{EM} cells in PDT/Mal-NPs plus anti-PD-L1 group was much higher than that in mice treated with either surgery only or surgery plus anti-PD-L1, or PDT/Mal-NPs (Figure S13, Supporting Information). In contrast, the frequency of T_{CM} cells in PDT/Mal-NPs plus anti-PD-L1 was much lower than that of the other three groups, indicating long-term immune memory protection. Combination of PDT/Mal-NPs and anti-PD-L1 substantially inhibited tumor growth compared with other treatments. Importantly, this memory immune response also prolonged survival time. Around 66.7% of mice in the PDT/Mal-NPs/anti-PD-L1 group survived for 90 days, while all mice in surgery and PDT/Mal-NPs controls died within 40 days (Figure S13f, Supporting Information).

In this study, we designed self-assembled polymeric nanoparticles with neoantigen harvesting and self-adjuvanted capabilities for personalized tumor immunotherapy. Our data indicate that these nanoparticles harvest neoantigens from perished cells to form SeaMac nanovaccines, which can induce DC maturation, present neoantigens to $CD8^+$ T cells with high efficiency, and augment the effect of $CD8^+$ CTL activation. These activated $CD8^+$ T cells have proven effective in inhibiting primary and distant tumor growth and prolonging the survival time of tumor-bearing mice.

Checkpoint inhibitors, such as anti-PD-L1 antibody and anti-CTLA-4 antibody, have greatly changed the treatment and prognosis of cancers, especially melanoma. However, only a minority of solid tumors respond to immune check inhibitors. Nanoparticle-based multi-mode therapies, in combination with immunotherapy, have achieved abscopal effects in various tumors.[10,17,23] However, the synergistic effect of these combination strategies usually requires commercial adjuvants (e.g., CpG, PIC, R837) or immune checkpoint inhibitors (e.g., anti-PD-L1, anti-CTLA-4, anti-PD-1 antibodies), which inevitably increases the complexity and cost of cancer treatment. In our study, SeaMac nanovaccines can function as an adjuvant to evoke abscopal effects in both CT26 and B16-F10 tumors in the absence of additional immunoactivators. Without the help of anti-PD-L1 or anti-CTLA-4 antibody, the evoked $CD8^+$ IFN-γ^+ T cells by PDT+Mal-NPs should play a key role in inducing "abscopal effect", because immune checkpoint inhibitors with other treatments substantially improve abscopal response rates but not necessarily with induced "abscopal effect."

Furthermore, tumor heterogeneity often limits the effectiveness of cancer therapy, which may explain why traditional approaches based on administration of one or several "selected" neoantigens fail to improve immunotherapeutic responses.[24] Min et al. engineered the biodegradable polymer poly lactic-co-glycolic acid (PLGA) nanoparticles with different functional groups for neoantigen capture and found that the combination of Mal AC-NPs with αPD-1 antibody facilitated the abscopal effect.[10] The *ex vivo* stimulation studies of splenocytes showed that the captured neoantigens can induce neoantigen-specific T cell proliferation and activation. This indicates that antigen-capturing nanoparticles for cancer immunotherapy offer a promising strategy for personalized therapy. It means that the neoantigens captured by Mal-NPs may also evoke

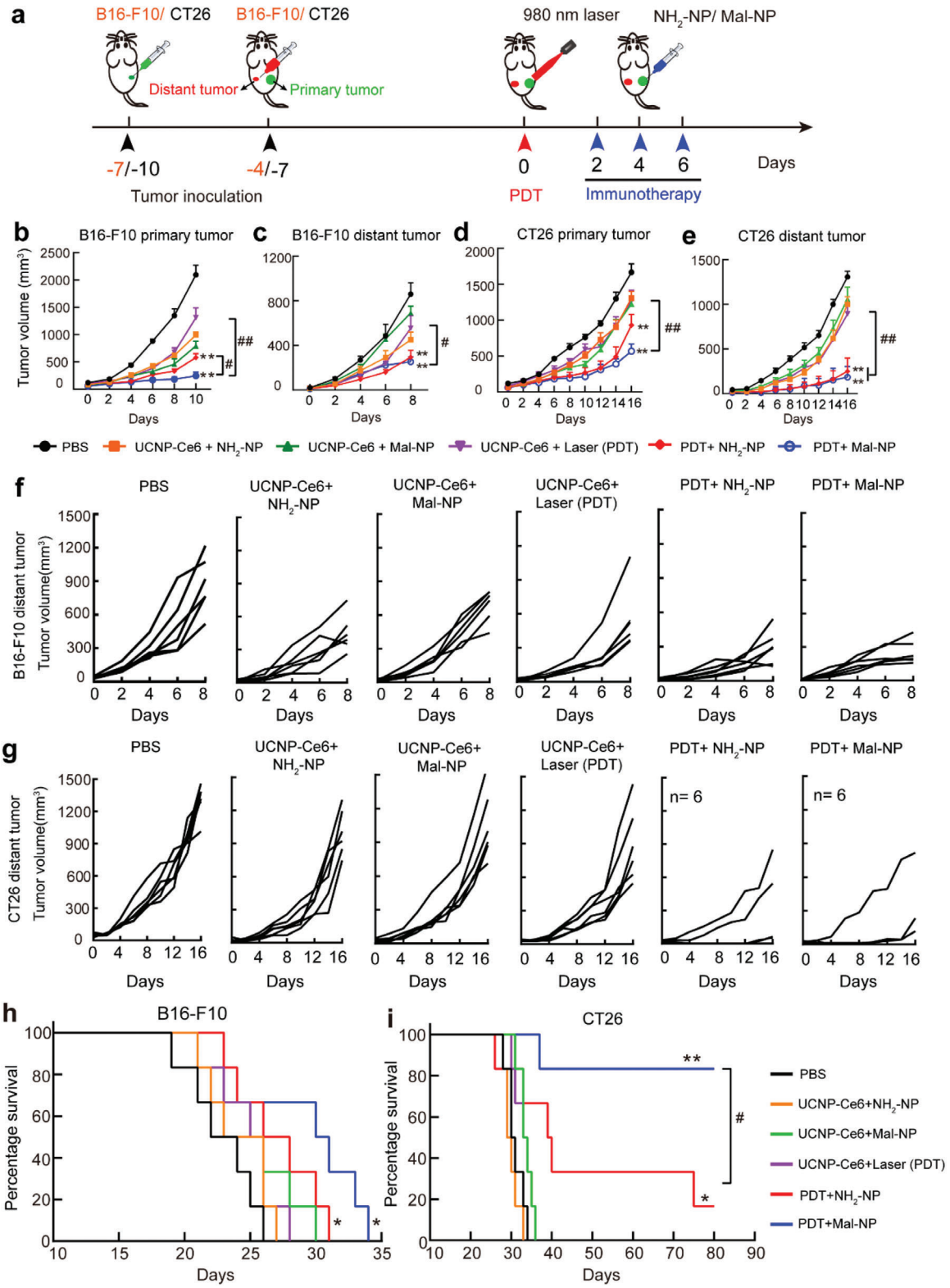

Figure 5. Mal-NPs improves *in vivo* abscopal effects of B16-F10 and CT26 tumors. a) Schematic timeline of abscopal effect evaluation. b,c) Tumor growth curves of the primary tumor (b) and distant tumor (c) in the B16 F10 tumor model. d,e) Tumor growth curves of the primary tumor (d) and distant tumor (e) in the CT26 tumor model. f) Growth curves of untreated (secondary) tumors in individual mice in (c). g) Growth curves of untreated (secondary) tumors in individual mice in (e). h) The survival rate of the mice in the B16-F10 tumor model. i) The survival rate of the mice in the CT26 tumor model. Data represent means ± s.e.m. ($n = 6$ mice per group; asterisk: PBS versus other treatments, $^{*}p < 0.05$; $^{**}p < 0.01$; hash: two different groups, $^{\#}p < 0.05$; $^{\#\#}p < 0.01$; tumor volume: One-way ANOVA analysis with Tukey test; survival rate: long-rank test).

neoantigen-specific immune response, eliminating time-consuming *de novo* sequencing and artificial synthesis. Moreover, PLGA NPs were selected as delivery systems due to their biocompatibility and biodegradability.[10] Different from PLGA NPs, Mal-NPs has intrinsic adjuvanticity, since C7A (the inner core of Mal-NPs) can potently promote DC maturation through STING without the need for additional adjuvants, providing a simple and low-cost personalized cancer immunotherapy.

3. Conclusion

Unlike conventional methods, our SeaMac nanovaccines provide the immune system with a wide variety of neoantigens and DAMPs in an individual-specific manner, evoking potent cellular immune responses. We speculate that SeaMac nanovaccines may allow cancer drugs to be delivered to tumors with unprecedented precision, triggering a synergistic effect of chemotherapy and immunotherapy. Since PEG has been approved by the U.S. Food and Drug Administration for clinical use, the SeaMac strategy may hold high potential for personalized immunotherapy in clinical trials with short production duration, low cost, and widespread applications.

Supporting Information

Supporting Information is available from the Wiley Online Library or from the author.

Acknowledgements

Z.L. and T.H. contributed equally to this work. Animal experiments were approved by the Institutional Animal Care and Treatment Committee of Sichuan University. This work is supported by the National Key & Program of China (No. 2018YFA0902600), the National Natural Science Foundation of China (21635002, 21771135, 21871071), the Ministry of Education, Singapore (MOE2017-T2-2-110), the Agency for Science, Technology and Research (A*STAR) (Grant NO. A1883c0011 and A1983c0038), and National Research Foundation, the Prime Minister's Office of Singapore under its NRF Investigatorship Programme (Award No. NRF-NRFI05-2019-0003). The authors thank M. J. Y. Ang for helpful discussion.

Conflict of Interest

The authors declare no conflict of interest.

Keywords

abscopal effect, nanovaccine, neoantigen-harvesting, self-adjuvanted, tumor immunotherapy

Received: November 27, 2020
Published online: December 18, 2020

[1] P. Hunter, *EMBO Rep.* **2017**, *18*, 1889.
[2] a) P. W. Kantoff, C. S. Higano, N. D. Shore, E. R. Berger, E. J. Small, D. F. Penson, C. H. Redfern, A. C. Ferrari, R. Dreicer, R. B. Sims, *N. Engl. J. Med.* **2010**, *363*, 411; b) F. S. Hodi, S. J. O'Day, D. F. McDermott, R. W. Weber, J. A. Sosman, J. B. Haanen, R. Gonzalez, C. Robert, D. Schadendorf, J. C. Hassel, *N. Engl. J. Med.* **2010**, *363*, 711; c) E. B. Garon, N. A. Rizvi, R. Hui, N. Leighl, A. S. Balmanoukian, J. P. Eder, A. Patnaik, C. Aggarwal, M. Gubens, L. Horn, *N. Engl. J. Med.* **2015**, *372*, 2018; d) J. A. Fraietta, S. F. Lacey, E. J. Orlando, I. Pruteanu-Malinici, M. Gohil, S. Lundh, A. C. Boesteanu, Y. Wang, R. S. O'Connor, W.-T. Hwang, *Nat. Med.* **2018**, *24*, 563.
[3] I. Melero, G. Gaudernack, W. Gerritsen, C. Huber, G. Parmiani, S. Scholl, N. Thatcher, J. Wagstaff, C. Zielinski, I. Faulkner, *Nat. Rev. Clin. Oncol.* **2014**, *11*, 509.
[4] M. E. Dudley, J. R. Wunderlich, P. F. Robbins, J. C. Yang, P. Hwu, D. J. Schwartzentruber, S. L. Topalian, R. Sherry, N. P. Restifo, A. M. Hubicki, *Science* **2002**, *298*, 850.
[5] a) S. Kreiter, M. Vormehr, N. Van de Roemer, M. Diken, M. Löwer, J. Diekmann, S. Boegel, B. Schrörs, F. Vascotto, J. C. Castle, *Nature* **2015**, *520*, 692; b) E. Alspach, D. M. Lussier, A. P. Miceli, I. Kizhvatov, M. DuPage, A. M. Luoma, W. Meng, C. F. Lichti, E. Esaulova, A. N. Vomund, *Nature* **2019**, *574*, 696.
[6] a) P. A. Ott, Z. Hu, D. B. Keskin, S. A. Shukla, J. Sun, D. J. Bozym, W. Zhang, A. Luoma, A. Giobbie-Hurder, L. Peter, *Nature* **2017**, *547*, 217; b) E. Tran, S. Turcotte, A. Gros, P. F. Robbins, Y.-C. Lu, M. E. Dudley, J. R. Wunderlich, R. P. Somerville, K. Hogan, C. S. Hinrichs, *Science* **2014**, *344*, 641; c) D. B. Keskin, A. J. Anandappa, J. Sun, I. Tirosh, N. D. Mathewson, S. Li, G. Oliveira, A. Giobbie-Hurder, K. Felt, E. Gjini, *Nature* **2019**, *565*, 234; d) E. Tran, M. Ahmadzadeh, Y.-C. Lu, A. Gros, S. Turcotte, P. F. Robbins, J. J. Gartner, Z. Zheng, Y. F. Li, S. Ray, *Science* **2015**, *350*, 1387.
[7] M. Luo, H. Wang, Z. Wang, H. Cai, Z. Lu, Y. Li, M. Du, G. Huang, C. Wang, X. Chen, *Nat. Nanotechnol.* **2017**, *12*, 648.
[8] R. L. Sabado, S. Balan, N. Bhardwaj, *Cell Res.* **2017**, *27*, 74.
[9] L. Miao, L. Li, Y. Huang, D. Delcassian, J. Chahal, J. Han, Y. Shi, K. Sadtler, W. Gao, J. Lin, *Nat. Biotechnol.* **2019**, *37*, 1174.
[10] Y. Min, K. C. Roche, S. Tian, M. J. Eblan, K. P. McKinnon, J. M. Caster, S. Chai, L. E. Herring, L. Zhang, T. Zhang, *Nat. Nanotechnol.* **2017**, *12*, 877.
[11] M. M. Gubin, M. N. Artyomov, E. R. Mardis, R. D. Schreiber, *J. Clin. Invest.* **2015**, *125*, 3413.
[12] D. V. Krysko, A. D. Garg, A. Kaczmarek, O. Krysko, P. Agostinis, P. Vandenabeele, *Nat. Rev. Cancer* **2012**, *12*, 860.
[13] P. A. Roche, K. Furuta, *Nat. Rev. Immunol.* **2015**, *15*, 203.
[14] U. H. von Andrian, T. R. Mempel, *Nat. Rev. Immunol.* **2003**, *3*, 867.
[15] D. T. O'Hagan, N. M. Valiante, *Nat. Rev. Drug Discovery* **2003**, *2*, 727.
[16] R. Maldonado-López, T. De Smedt, P. Michel, J. Godfroid, B. Pajak, C. Heirman, K. Thielemans, O. Leo, J. Urbain, M. Moser, *J. Exp. Med.* **1999**, *189*, 587.
[17] Q. Chen, L. Xu, C. Liang, C. Wang, R. Peng, Z. Liu, *Nat. Commun.* **2016**, *7*, 1.
[18] D. Shae, K. W. Becker, P. Christov, D. S. Yun, A. K. Lytton-Jean, S. Sevimli, M. Ascano, M. Kelley, D. B. Johnson, J. M. Balko, *Nat. Nanotechnol.* **2019**, *14*, 269.
[19] H. Liang, L. Deng, Y. Hou, X. Meng, X. Huang, E. Rao, W. Zheng, H. Mauceri, M. Mack, M. Xu, *Nat. Commun.* **2017**, *8*, 1.
[20] F. Sallusto, D. Lenig, R. Förster, M. Lipp, A. Lanzavecchia, *Nature* **1999**, *401*, 708.
[21] I. M. Desar, J. F. Jacobs, C. A. Hulsbergen-vandeKaa, W. J. Oyen, P. F. Mulders, W. T. van der Graaf, G. J. Adema, C. M. van Herpen, I. J. de Vries, *Int. J. Cancer* **2011**, *129*, 507.
[22] E. J. Wherry, V. Teichgräber, T. C. Becker, D. Masopust, S. M. Kaech, R. Antia, U. H. Von Andrian, R. Ahmed, *Nat. Immunol.* **2003**, *4*, 225.
[23] a) J. Xu, L. Xu, C. Wang, R. Yang, Q. Zhuang, X. Han, Z. Dong, W. Zhu, R. Peng, Z. Liu, *ACS Nano* **2017**, *11*, 4463; b) Q. Chen, J. Chen, Z. Yang, J. Xu, L. Xu, C. Liang, X. Han, Z. Liu, *Adv. Mater.* **2019**, *31*, 1802228; c) C. He, X. Duan, N. Guo, C. Chan, C. Poon, R. R. Weichselbaum, W. Lin, *Nat. Commun.* **2016**, *7*, 1.
[24] C. J. Melief, T. van Hall, R. Arens, F. Ossendorp, S. H. van der Burg, *J. Clin. Invest.* **2015**, *125*, 3401.

